Thermal metamaterial for convergent transfer of conductive heat with high efficiency

Xiangying Shen, Chaoran Jiang, Ying Li, and Jiping Huang

Citation: Applied Physics Letters **109**, 201906 (2016); doi: 10.1063/1.4967986
View online: http://dx.doi.org/10.1063/1.4967986
View Table of Contents: http://scitation.aip.org/content/aip/journal/apl/109/20?ver=pdfcov
Published by the AIP Publishing

Thermal metamaterial for convergent transfer of conductive heat with high efficiency

Xiangying Shen,[1,2,a),b)] Chaoran Jiang,[1,2,a)] Ying Li,[3] and Jiping Huang[1,2,c)]
[1]*Department of Physics, State Key Laboratory of Surface Physics, and Key Laboratory of Micro and Nano Photonic Structures (MOE), Fudan University, Shanghai 200433, China*
[2]*Collaborative Innovation Center of Advanced Microstructures, Nanjing 210093, China*
[3]*Department of Mechanics and Engineering Science, Fudan University, Shanghai 200433, China*

(Received 11 August 2016; accepted 5 November 2016; published online 17 November 2016)

It is crucially important to focus conductive heat in an efficient way, which has received much attention in energy science (say, solar cells), but is still far from being satisfactory due to the diffusive (divergent) nature of the heat. By developing a theory with hybrid transformations (rotation and stretch-compression), here we provide theoretical and experimental evidences for a type of thermal metamaterial called thermal converger. The converger is capable of convergently conducting heat in contrast to the known divergent behavior of heat diffusion, thus yielding a large heating region with high temperatures close to the heat source (high efficiency). The thermal converger further allows us to design a thermal grating—a thermal counterpart of optical grating. This work has relevance to heat focus with high efficiency, and it offers guidance both for efficient heat transfer and for designing thermal-converger-like metamaterials in other fields, such as electrics/magnetics, electromagnetics/optics, acoustics, and particle diffusion. *Published by AIP Publishing.*
[http://dx.doi.org/10.1063/1.4967986]

Focusing conductive (diffusion) heat in an efficient way is crucial in energy science including solar cells[1] and thermoelectric effects.[2] In 2006, two research groups established the transformation optics theory,[3,4] which provides a powerful tool to control electromagnetic waves.[5,6] Soon, this theoretical approach has been extended to acoustics,[7] electrics,[8] magnetics,[9] elastic waves,[10] and even matter waves.[11] Inspired by transformation optics, some researchers extended the transformation mapping theory to the domain of thermal conduction.[12] Recently, physicists designed a lot of thermal metamaterials with different thermal characteristics.[13–30] Nowadays, thermal metamaterials (including metamaterials) based on the transformation mapping theory have aroused big interests in the science community.[12,15–18,24–29,31–39]

As known to us, there are three basic transformations: translation, rotation, and stretch-compression. In this work, after developing a theory of hybrid transformation thermotics, we adopt rotation and stretch-compression to introduce a concept of thermal converger that is capable of convergingly conducting heat in contrast to the known diverging behavior of heat conduction, thus causing a large heating region with high temperatures close to the heat source. Moreover, the converging effect can be utilized to convert a line heat source into a point, which helps to design a kind of thermal grating—the thermal counterpart of optical grating. To this end, we shall report that the effect can be confirmed by finite-element simulations and experiments by utilizing commercially available homogeneous materials according to the effective medium theory.[40] The converger implies that the theory of hybrid transformation thermotics could be a useful theoretical method for heat energy manipulations, and its structure could also offer hints on how to control heat flow at will and on how to design thermal-converger-like metamaterials in other fields, such as electromagnetics/optics, electrics/magnetics, acoustics, and particle diffusion.

A hybrid transformation theory relies on the material parameter of thermal conductivity in the field of thermotics. In fact, it holds the same in other fields like electromagnetics/optics, electrics/magnetics, and acoustics as long as one replaces thermal conductivity with electric permittivity and magnetic permeability (in electromagnetics/optics or electrics/magnetics) or mass density and bulk modulus (in acoustics) accordingly. To proceed, let us start by considering a steady-state thermal conduction equation without the heat source. We should notice that the following derivation is correct but limited to transformations between orthonormal bases or for scalars only. Otherwise, additional terms will appear in the equation. Fortunately, the conductivity of the host is always considered as scalar, which warrants the derivation valid. The domain equation satisfies $\nabla \cdot \tilde{\kappa} \nabla T = 0$, where $\tilde{\kappa}$ is a thermal conductivity and T represents the temperature distribution in a two-dimensional Cartesian system with coordinates (x, y). This equation keeps form invariance under the coordinate transformation. In the deformed space (x', y'), the thermal conductivity $\tilde{\kappa}$ changes to

$$\tilde{\kappa}' = \frac{\mathbf{J}\tilde{\kappa}\mathbf{J}^{\mathrm{t}}}{\det(\mathbf{J})}, \tag{1}$$

where $\mathbf{J}$ is the Jacobian transformation matrix between the distorted and original coordinates, $\mathbf{J}^{\mathrm{t}}$ is the transposed matrix of $\mathbf{J}$, and $\det(\mathbf{J})$ is the determinant of $\mathbf{J}$. The $\mathbf{J}$ allows people to realize the transformation effect by tailoring the materials' thermal conductivities appropriately. So, we write the second-order tensor of transformed thermal conductivity $\tilde{\kappa}'$

[a)]X. Shen and C. Jiang contributed equally to this work.
[b)]Electronic mail: 13110190068@fudan.edu.cn
[c)]Electronic mail: jphuang@fudan.edu.cn

as the product of a transformation matrix (T) and the original conductivity ($\tilde{\kappa}$)

$$\tilde{\kappa}' = \tilde{\kappa}\mathrm{T} = \kappa_0\mathrm{T} = \begin{pmatrix} \kappa_{xx} & \kappa_{xy} \\ \kappa_{xy} & \kappa_{yy} \end{pmatrix}\kappa_0. \tag{2}$$

Here, for simplification, we have set $\tilde{\kappa}$ to be isotropic and homogenous, $\tilde{\kappa} = \kappa_0$. In particular, the transformation matrix T simultaneously represents one, two, or three of the basic transformations: translation, rotation, and stretch-compression.

When a translation transformation is applied to the system, there exists $\mathrm{J} = I$, where I is the identity matrix. It is intuitively obvious that the translation transformation exerts no influence to the whole system. As far as a rotation transformation $R(\theta)$ is concerned, it has a Jacobian matrix as

$$\begin{pmatrix} \cos\theta & \sin\theta \\ -\sin\theta & \cos\theta \end{pmatrix}.$$

The matrix can be used to rotate the principle axis by an angle of θ. Nevertheless, if the parameter of a material is a constant, the transformation matrix T is also an identity matrix, which has no effect on the original thermal conductivity. Next, for a stretch-compression transformation, we set n and m as the compression ratio of coordinates x and y, respectively. Either $n > 1$ or $m > 1$ means stretching the space. Otherwise, a compression transformation is applied. Then, we obtain the corresponding transformation matrix

$$\mathrm{T} = \begin{pmatrix} \frac{n}{m} & 0 \\ 0 & \frac{m}{n} \end{pmatrix}. \tag{3}$$

It should be noticed that one can stretch or compress the space along x or y direction. However, it can be derived that stretching coordinate y is equivalent to the compressing coordinate x because of

$$R\left(\frac{\pi}{2}\right)\begin{pmatrix} n & 0 \\ 0 & \frac{1}{n} \end{pmatrix}R\left(\frac{\pi}{2}\right)^{\mathrm{t}}\det{}^{-1}\left(R\left(\frac{\pi}{2}\right)\right) = \begin{pmatrix} \frac{1}{n} & 0 \\ 0 & n \end{pmatrix}.$$

The heat flow can be concentrated towards the vertical direction of the compression. That is, when $m < 1$, the heat energy will be focused along the x axis. Now, if we rotate the space with an angle of θ, the compression direction will rotate θ, too. When combined with the compression, now the rotation is crucial for controlling the conduction of heat. The combined transformations provide us a method for converging the heat flow by adjusting the concentrating direction. Then, we write the conductivity tensor as

$$\mathrm{T} = \begin{pmatrix} n\cos^2\theta + \frac{1}{n}\sin^2\theta & \frac{1}{n}\sin\theta\cos\theta - n\sin\theta\cos\theta \\ \frac{1}{n}\sin\theta\cos\theta - n\sin\theta\cos\theta & \frac{1}{n}\cos^2\theta + n\sin^2\theta \end{pmatrix}, \tag{4}$$

where θ is a function of the coordinate y. In the case of $\theta = s(y)$, if the device has a height, H, and is located at the origin of the coordinate plane, then we set $\theta = s(y) = y\frac{\pi}{H}$. More explicitly, for the top and bottom edges, $y = \pm H/2$, we have $s(y) = \pm\pi/2$. Thus, the tensor turns to diag$(1/n, n)$.

If n is big enough, the above matrix leads to the stretch (or compression) transformation of y (or x) coordinates. As a result, the heat can hardly conduct from left to right, but flow downward or upward to the central region. On the other hand, for the middle part of the material, say, $y = 0$, there is $s(y) = \pi$. The tensor is reduced to diag$(n, 1/n)$. More

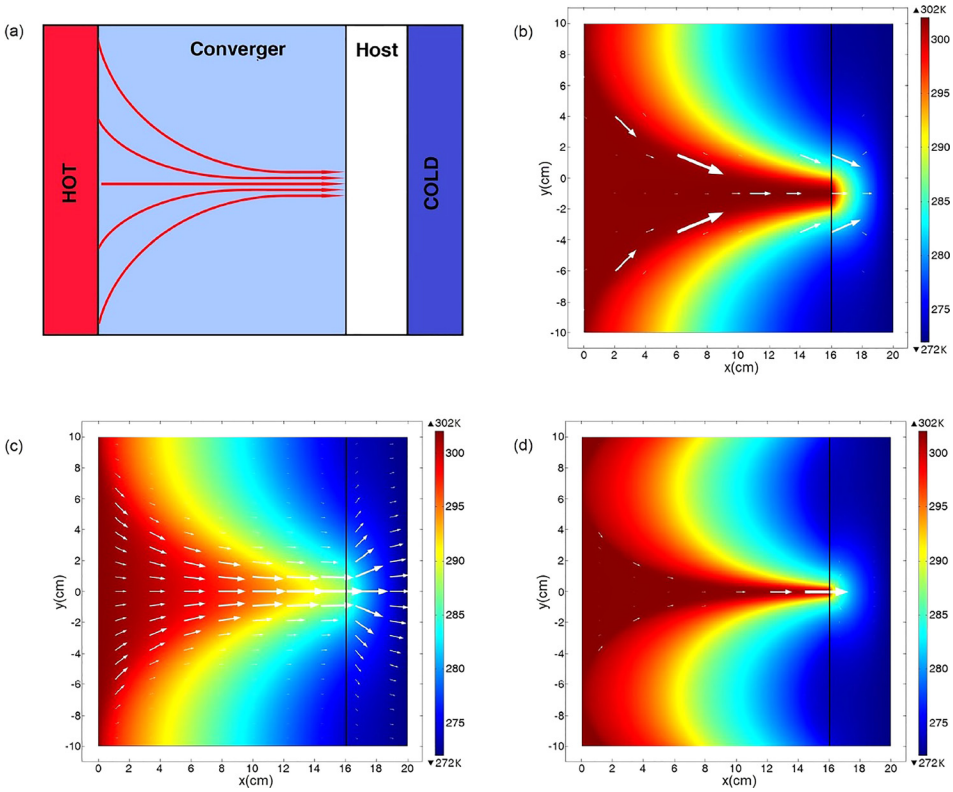

FIG. 1. (a) Schematic graph showing a thermal converger aside a host between hot and cold sources. Arrowed lines represent heat flow that converges in the device. (b)–(d) Finite-element simulation results of temperature distribution in the thermal converger separated from the host by a vertical line, according to Eq. (4). The left (or right) boundary is set at a high (or low) temperature $T_H = 302\,\mathrm{K}$ (or $T_L = 272\,\mathrm{K}$); the upper and lower boundaries are associated with thermal isolation. The white arrow denotes the heat flow, and its size is proportional to the magnitude of heat flux at the corresponding positions in each panel. Parameters: (b) $n = 200$ and $\theta = s(y) = (1/H)\pi y$; (c) $n = 5$ and $\theta = s(y) = (1/H)\pi y$; (d) $n = 200$ and $\theta = s(y) = (3/2H)\pi y$.

interestingly, according to the above equation, with a higher value of n, the conductivity component κ_{xx} would be much larger than κ_{yy}, which may cause a super-transferring phenomenon in the middle region of the material. Heat energy will be restricted to conduct along the x axis and hardly diffuse in the y direction. Taking the above discussions into account, the $s(y)$ makes the material behave as a thermal converger [see Fig. 1(a)], since the heat energy would be converged to propagate in the middle part. Unlike some conventional design (e.g., using a common pure metal like copper), the heat energy under our consideration can not divergingly diffuse as required by Fourier's law, but convergingly conduct along a pre-determined path. Hence, we call the device "thermal converger."

To illustrate the behaviour of the thermal converger, we perform finite-element simulations based on the commercial software COMSOL Multiphysics.[41] The simulations of this section are performed in a box with height $H = 20\,\text{cm}$ and width $L = 20\,\text{cm}$. We set the temperature $T_H = 302\,\text{K}$ and $T_L = 272\,\text{K}$ at the left and right boundaries of the box, respectively. The upper and lower edges are kept as thermal isolation. As shown in Fig. 1(b), a 20 cm $\times$ 16 cm converger material is located aside a host whose thermal conductivity is normalized to 1 W/mK. For simplification, we set θ to be proportional to y, $\theta = s(y) = (1/H)\pi y$. Fig. 1(b) presents the performance of thermal converger, and the temperature distribution is indicated by the color surface. Clearly, unlike the common conduction, heat flow is converged to a small area on the interface. It should also be noted that due to a high value of $n = 200$, a super-transferring phenomenon takes place in the middle region of the device. That is, along the $y = 0$ axis, there exists a large heating region with high temperatures close to the heat source.

In addition, we plot Figs. 1(c) and 1(d) to show how the stretch-compression and rotation affect the converging effect, respectively. In Fig. 1(c), the $s(y)$ function keeps unchanged and the compression ratio $n = 5$. In this case, although the heat flow is converged, there exists evident temperature gradient in the original super-transferring region as shown in Fig. 1(b). As a result, the temperature at the converge point is much smaller than the heat source. For the case displayed in Fig. 1(d), n holds the same value as that of Fig. 1(b), but we set $s(y) = 3/2H\pi y$ instead. Therefore, the strong limitation of thermal conduction at the top or bottom edges becomes weakened. That is, at those places heat tends to conduct more easily.

The thermal conductivities of thermal converger are not only anisotropic but also inhomogeneous, which lead to a challenge for fabricating such materials. The transformation of the thermal converger consists of both stretch-compression and rotation; we may express the converger's thermal conductivity as $R(\theta)\text{diag}(n, 1/n)R^{-1}(\theta)$. To realize such conductivity, we decide to resort to the laminated structure similarly to the previous work (see Ref. 30). As shown in Fig. 2, the converger (metamaterial) with dimensions $H = 18.75\,\text{cm}$ and $L = 16\,\text{cm}$ is divided into 19 layers. It should be noted that every layer has a height of 1 cm, except for the central layer, whose height is 0.75 cm. Next, since the rotation transformation can be achieved by rotating the principle axis of a

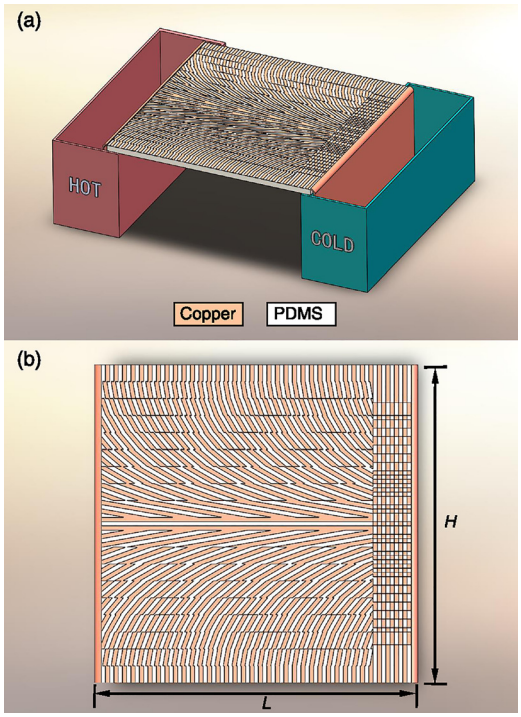

FIG. 2. (a) The blueprint of our experimental sample connecting the heat and cold sources provided by heat bath. We fabricate the sample by chemically etching a copper plate and filling in polydimethylsiloxane (PDMS) accordingly. (b) displays a front view of the sample. The converger (or host) region has a width of 16 cm (or 2.25 cm). Other parameters: $L = 18.75\,\text{cm}$ and $H = 18.75\,\text{cm}$.

system, each layer's principle axis is restricted to rotate with a fixed θ, varying from $-\frac{\pi}{2}$ to $\frac{\pi}{2}$. Thus, the angle difference between principle axes of every two connective layers is $\pi/18$. Therefore, for each layer, the hybrid transformation is reduced to a compression and a rotation with a certain angle. To obtain the diagonalized thermal conductivity generated by compression, we resort to the effective medium theory.[40] Now, we can fabricate the materials with such thermal conductivities by using an alternation of two homogeneous isotropic sub-layers with the thicknesses of d_A and d_B and the conductivities of κ_A and κ_B. Then, we obtain

$$\kappa_{xx} = \frac{\kappa_A + \eta\kappa_B}{1+\eta}, \qquad \frac{1}{\kappa_{yy}} = \frac{1}{1+\eta}\left(\frac{1}{\kappa_A} + \frac{\eta}{\kappa_B}\right), \tag{5}$$

where $\eta = d_B/d_A$. Owing to the reciprocal relationship between κ_{xx} and κ_{yy}, $\kappa_{xx} = 1/\kappa_{yy} = n$, the above approximation would be strictly correct only when $\kappa_A\kappa_B = 1$. Therefore, the least perturbation can be achieved by making $\kappa_A\kappa_B = \kappa_0^2$. Here, κ_0 is the conductivity of the host, and it should have the same determinant value ($\det(\mathrm{T}) = 1$ in Eq. (4)) as the converger. As aforementioned, the compression and stretch transformations can be achieved by the alternating laminated structures. For the sake of preserving the same determinant of conductivity, the same spatial composition as shown in the right part of Fig. 2(b) should be adopted to construct the host material (the host medium with dimensions: $H = 18.75\,\text{cm}$; $L = 2.25\,\text{cm}$). In the simulations as shown in Fig. 3(a), we set $\eta = 1$ and take the alternating sub-layers of copper ($\kappa_{cu} = 394\,\text{W/mK}$) and

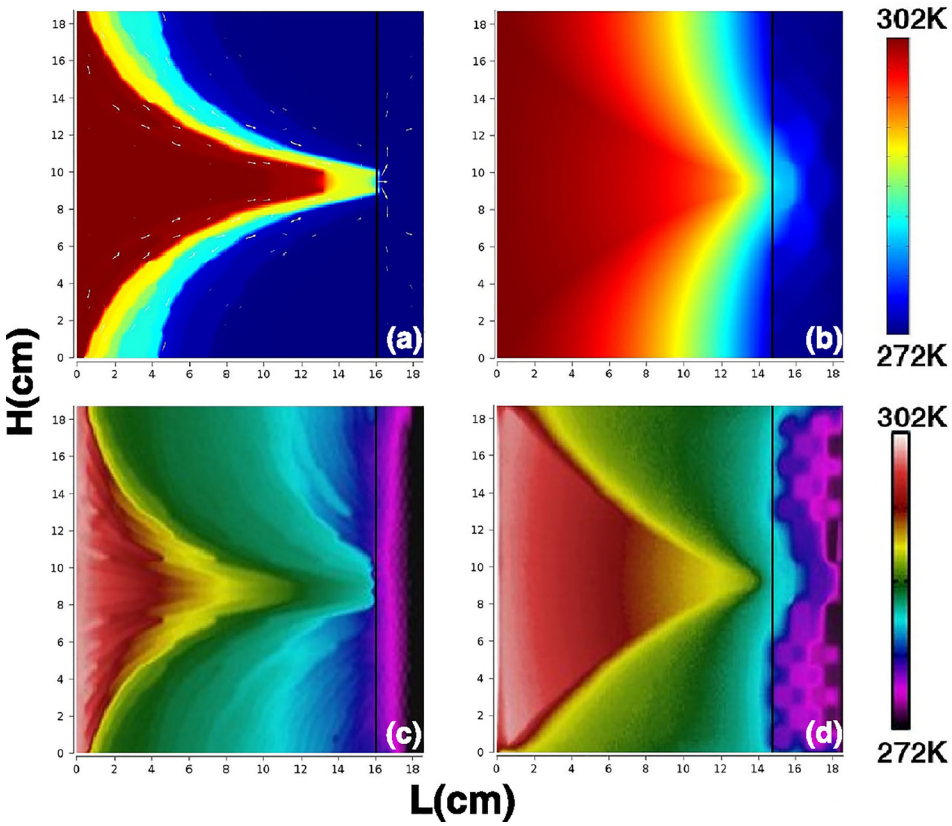

FIG. 3. (a) Finite-element simulation results of the temperature distribution in the structure displayed in Fig. 2, according to the effective medium theory. (b) Same as (a), but in a reference sample, namely, the converging part is replaced with a pure copper funnel embedded in PDMS. The white arrow represents the flow of heat, and its size is proportional to the magnitude of heat flux at the corresponding positions in (a) or (b). (c) The experimental measurement results of temperature distribution in our experimental sample is shown in Fig. 2. (d) Same as (c), but in a comparison sample. The vertical line in (a) and (c) separates the converger from the host.

polydimethylsiloxane ($\kappa_{PDMS} = 0.15$ W/mK). When compared with Fig. 3(b), a comparison simply composed by replacing the converger with the pure copper funnel embedded in PDMS, Fig. 3(a) shows that the converge works satisfactorily, which displays a high and uniform temperature distribution in a large region indeed. In other words, it is reasonable for us to design the converger material by resorting to the effective medium theory.

Fig. 2 displays our experimental design: the device is made from a 0.5 mm-thick copper plate; the alternating and rotating structures are achieved by chemically etching holes on the plate. Polydimethylsiloxane is filled in the holes to provide a high enough value of compression ratio due to its much smaller conductivity than that of copper. Moreover, a 0.01 mm-thick polydimethylsiloxane film on the top of the copper is nearly "black" for the wavelengths seen by the thermal camera in contrast to the reflective copper itself. Thus, there is no need for additional coating of the surface in order to make the device visible for the camera. A stable heat source is served by a tank filled with hot water, whose heat capacitance is much higher than the composite plate. The right-hand side of the device is immersed in a same tank filled with an ice-water mixture. The room temperature is about 288 K, and the temperature of the hot water is 302 K. The whole device is placed on a 2 cm-thick plate of expanded polystyrene.

Fig. 3(c) shows the experimental measurement results of the prototype device. As denoted by the color surface captured by the Flir E60 thermal camera, the temperature distribution indicates that the heat flow is converged indeed, and that there is a large heating region with a high temperature. Clearly, in contrast to the referenced sample, the converging effect is much better, since the pattern of temperature distribution is more diffusive in the copper funnel case, and the temperature in PDMS is higher. Nevertheless, compared with the simulation results [Fig. 3(a)] for the large heating region with high temperatures in the middle region, the heating region detected in experiment [Fig. 3(c)] appears to be qualitatively same, but slightly different due to the dissipation of radiation and convection.

Based on the converger material, we further propose a class of thermal grating. Details are as follows: When $\theta > \frac{\pi}{2}$ in Eq. (4), the thermal conductivities will change in a periodic pattern, which causes heat conduction in such a material to be similar to the light resolved in an optical grating. Thus, we achieve a kind of thermal grating, which can be simply obtained by arraying thermal convergers periodically. For simulations, we set $\theta = s(y) = y\frac{a\pi}{H}$, where a is the number of cycles. Figs. 4(a) and 4(b) show the simulation result of such a thermal grating. Clearly, the thermal grating can be used to heat some specific points at its boundary on the right. In other words, it lets thermal energy converge and pass through the chosen "holes." The most probable application of the thermal grating as we consider is making illusion in order to change the linear heat source into point heat source and providing unexplored idea or approach for transforming the geometry shape of the heat source.

We have developed a theory of hybrid transformation thermotics for a macroscopic manipulation of heat flow. As an application, we proposed a type of thermal metamaterial, the thermal converger in which heat convergingly conducts along a pre-designed path in contrast to the diverging behavior of heat conduction. Interestingly, the converger yields a large heating region with high temperatures close to the heat source. This performance is much better than that of the pure metallic funnel embedded in a thermal isolator, and it is also

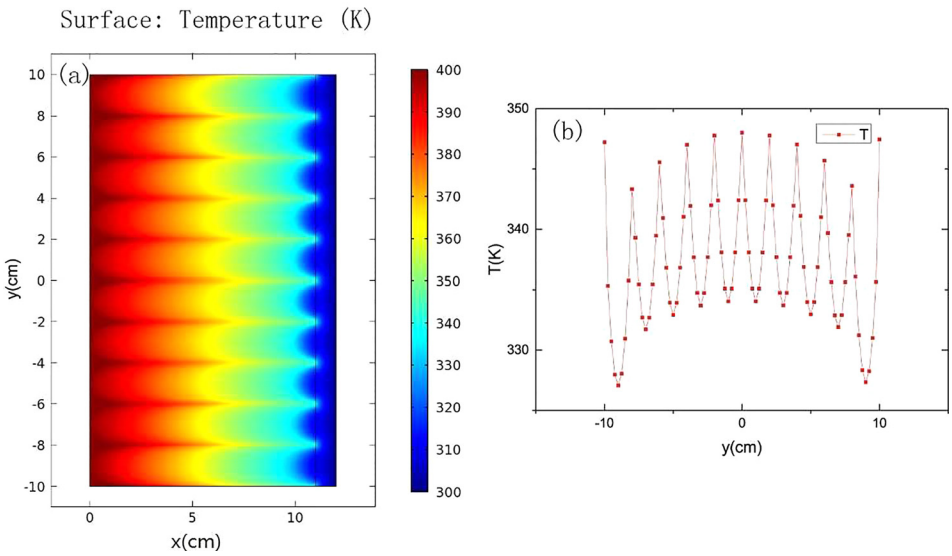

FIG. 4. Finite-element simulation results: (a) the temperature distribution of a thermal grating made from thermal convergers; (b) the values of temperature at $x = 11$ cm in (a). Parameters: $a = 10$.

confirmed by finite-element simulations and experiments. Based on the concept of thermal converger, we can also design a kind of thermal grating—the thermal counterpart of optical grating. In addition, the thermal converger has potential applications in many aspects, such as either thermal illusion for misleading infrared detection in military uses or heat preservation in designing combustors or furnaces with a high radiation power density in industry. This work is useful for heat focus with efficiency, and it provides guidance both for efficient heat transfer and for designing thermal-converger-like metamaterials in other fields.

We thank Dr. Zuhui Wu for helpful assistance and discussion. We acknowledge the financial support from the Science and Technology Commission of Shanghai Municipality under Grant No. 16ZR1445100.

[1]P. Wang, S. M. Zakeeruddin, J. E. Moser, M. K. Nasseruddin, T. Sekiguchi, and M. Gratzel, Nat. Mater. **2**, 402 (2003).
[2]V. R. Venkatasubramanian, E. Sivola, T. Colpitts, and B. O'Quinn, Nature **413**, 597 (2001).
[3]J. B. Pendry, D. Schurig, and D. R. Smith, Science **312**, 1780 (2006).
[4]U. Leonhardt, Science **312**, 1777 (2006).
[5]U. Leonhardt and T. G. Philbin, New J. Phys. **8**, 247 (2006).
[6]M. W. McCall, A. Favaro, P. Kinsler, and A. Boardman, J. Opt. **13**, 029501 (2011).
[7]H. Y. Chen and C. T. Chan, Appl. Phys. Lett. **91**, 183518 (2007).
[8]F. Yang, Z. L. Mei, T. Y. Jin, and T. J. Cui, Phys. Rev. Lett. **109**, 053902 (2012).
[9]F. Gömöry and A. Sanchez, Science **335**, 1466 (2012).
[10]N. Stenger, M. Wilhelm, and M. Wegener, Phys. Rev. Lett. **108**, 014301 (2012).
[11]S. Zhang, D. A. Genov, C. Sun, and X. Zhang, Phys. Rev. Lett. **100**, 123002 (2008).
[12]C. Z. Fan, Y. Gao, and J. P. Huang, Appl. Phys. Lett. **92**, 251907 (2008).
[13]H. Y. Xu, X. H. Shi, F. Gao, H. D. Sun, and B. L. Zhang, Phys. Rev. Lett. **112**, 054301 (2014).
[14]X. Y. Shen and J. P. Huang, Int. J. Heat Mass Transfer **78**, 1 (2014).
[15]T. C. Han, T. Yuan, B. W. Li, and W. C. Qiu, Sci. Rep. **3**, 1593 (2013).
[16]Y. Gao and J. P. Huang, EPL **104**, 44001 (2013).
[17]S. Narayana and Y. Sato, Phys. Rev. Lett. **108**, 214303 (2012).
[18]S. Guenneau, C. Amra, and D. Veynante, Opt. Express **20**, 8207 (2012).
[19]T. C. Han, J. Zhao, T. Yuan, D. Y. Lei, B. W. Li, and C. W. Qiu, Energy Environ. Sci. **6**, 3537 (2013).
[20]R. S. Kapadia and P. R. Bandaru, Appl. Phys. Lett. **105**, 233903 (2014).
[21]S. Guenneau and C. Amra, Opt. Express **21**, 6578 (2013).
[22]T. C. Han, X. Bai, J. T. L. Thong, B. W. Li, and C. W. Qiu, Adv. Mater. **26**, 1731 (2014).
[23]Y. Li, X. Y. Shen, Z. H. Wu, J. Y. Huang, Y. X. Chen, Y. S. Ni, and J. P. Huang, Phys. Rev. Lett. **115**, 195503 (2015).
[24]T. C. Han, X. Bai, D. Gao, J. T. Thong, B. W. Li, and C. W. Qiu, Phys. Rev. Lett. **112**, 054302 (2014).
[25]T. Yang, K. P. Vemuri, and P. R. Bandaru, Appl. Phys. Lett. **105**, 083908 (2014).
[26]R. Schittny, M. Kadic, S. Guenneau, and M. Wegener, Phys. Rev. Lett. **110**, 195901 (2013).
[27]Y. Ma, Y. Liu, M. Raza, Y. Wang, and S. He, Phys. Rev. Lett. **113**, 205501 (2014).
[28]J. Y. Li, Y. Gao, and J. P. Huang, J. Appl. Phys. **108**, 074504 (2010).
[29]M. Moccia, G. Castaldi, S. Savo, Y. Sato, and V. Galdi, Phys. Rev. X **4**, 021025 (2014).
[30]K. P. Vemuri and P. R. Bandaru, Appl. Phys. Lett. **103**, 133111 (2013).
[31]S. Narayana, S. Savo, and Y. Sato, Appl. Phys. Lett. **102**, 201904 (2013).
[32]Y. G. Ma, L. Lan, W. Jiang, F. Sun, and S. L. He, NPG Asia Mater. **5**, e73 (2013).
[33]E. M. Dede, T. Nomura, P. Schmalenberg, and J. S. Lee, Appl. Phys. Lett. **103**, 063501 (2013).
[34]T. Z. Yang, L. J. Huang, F. Chen, and W. K. Xu, J. Phy. D: Appl. Phy. **46**, 305102 (2013).
[35]X. He and L. Z. Wu, Appl. Phys. Lett. **102**, 211912 (2013).
[36]G. X. Yu, Y. F. Lin, G. Q. Zhang, Z. Yu, L. L. Yu, and J. Su, Front. Phys. **6**, 70 (2011).
[37]T. Z. Yang, X. Bai, D. L. Gao, L. Z. Wu, B. W. Li, J. T. L. Thong, and C. W. Qiu, Adv. Mater. **27**, 7752 (2015).
[38]X. Y. Shen, Y. Li, C. R. Jiang, Y. S. Ni, and J. P. Huang, Appl. Phys. Lett. **109**, 031907 (2016).
[39]X. Y. Shen, Y. Li, C. R. Jiang, and J. P. Huang, Phys. Rev. Lett. **117**, 055501 (2016).
[40]J. P. Huang and K. W. Yu, Phys. Rep. **431**, 87 (2006).
[41]See http://www.comsol.com/ for more detailed informations about the software.